Applied Nanoscience (2019) 9:825–833
https://doi.org/10.1007/s13204-018-0748-2

ORIGINAL ARTICLE

Gold nanoparticles as a factor of influence on doxorubicin–bovine serum albumin complex

N. A. Goncharenko[1] · O. L. Pavlenko[1] · O. P. Dmytrenko[1] · M. P. Kulish[1] · A. M. Lopatynskyi[2,3] · V. I. Chegel[2,3]

Received: 30 December 2017 / Accepted: 26 March 2018 / Published online: 4 April 2018

Abstract

The interaction between doxorubicin (Dox) and bovine serum albumin (BSA) complex with gold nanoparticles (AuNPs) was investigated by optical spectroscopy. The optical absorption of Dox and BSA solutions was studied. The formation of Dox–BSA complexes with a binding constant $K = 7.56 \times 10^6$ M^{-2} and the number of binding sites $n = 2$ was found out. With pH 6.9, the concentration of complexes is an order of magnitude lower than the concentration of unbound antibiotic molecules. Optical absorption in solutions of Dox–BSA conjugates in the presence of AuNPs undergoes a significant rearrangement, which manifests the changes in the magnitude of the hydrophobic interaction of BSA with Dox, changes in the conformational state of antibiotic, and, as a consequence, a plasmon-induced change in the mechanism of complex formation. The aggregation of the Dox–AuNPs conjugate depends on the presence and concentration of BSA and in the case of formation of the Dox–BSA complex is minimal.

Keywords Doxorubicin · Bovine serum albumin · Gold nanoparticles · Conformational state · Hydrophobic interaction · Electrostatic interaction · Localized surface plasmon resonance

Introduction

The effectiveness of chemotherapy for cancer treatment when using traditional antitumor drugs is insufficient, as it is accompanied by a number of adverse side effects. In the first place, all drug products of this direction are characterized by high total toxicity.

Particularly significant negative role is played by nephro-, hepato- and cardiotoxicity (Carvalho et al. 2014). In addition, due to the genetic variability of tumors, their cells acquire resistant properties to the action of these drugs. The characteristics of targeting, prolonged action, as well as the targeted delivery of drugs to pathological cells with minimal damage to biological structures on the way of their transport are low. Considered deficiencies of antitumor therapy are also inherent to one of the most common drugs—Dox.

Doxorubicin belongs to the anthracycline group of antibiotics due to its wide range of chemotherapeutic effects on malignant tumors and oncological diseases of the blood (Arcamone 1981; Krohn 1983; Zhong et al. 2013; Wang et al. 2013). Possibility of several mechanisms of anthracycline antibiotics action is assumed, among which intercalation in the DNA molecules with further inhibition of the synthesis of DNA, RNA and protein macromolecules is considered as one of the main. In addition, the possible mechanism of inhibition of the reproduction of tumor cells is the formation of free radicals that cause damage to DNA, cytoplasmic membrane, vascular endothelium and suppression of energy metabolism (Kalinkina 2004; Tevyashova 2014). To overcome the mechanisms of development of Dox resistance, to increase the selectivity of its action, and to ensure the detoxification associated with radical forms of oxygen, a variety of methods for the creation of modified drugs (prodrugs) through the attachment of chemical fragments to antitumor agents, synthesis of conjugates with metallic, semiconductor, carbon nanoparticles and metal ions are used (Meshalkin and Bgatova 2008; Dykman et al.

✉ A. M. Lopatynskyi
lop2000@ukr.net

[1] Faculty of Physics, Taras Shevchenko National University of Kyiv, 64/13, Volodymyrska Street, Kiev 01601, Ukraine

[2] V.E. Lashkaryov Institute of Semiconductor Physics, National Academy of Sciences of Ukraine, 41, Nauki Avenue, Kiev 03028, Ukraine

[3] Institute of High Technologies, Taras Shevchenko National University of Kyiv, 64/13, Volodymyrska Street, Kiev 01601, Ukraine

2008; Orel et al. 2016; Cataldo and Da Ros 2008; Montellano et al. 2011; Chen et al. 2012; Dellinger et al. 2013; Evstigneev et al. 2013; Dallavalle et al. 2014; Prylutskyy et al. 2014, 2015; Mosunov et al. 2017). Increasing the selectivity of drug perception by tumor cells in comparison with normal cells, while reducing the cytotoxicity caused by the occurrence of oxidative stress, involves the introduction into the body of not only antitumor agents, but also various antioxidant drugs acting as inhibitors of death of normal cells as a result of apoptosis (Durackova 2010; Lobo et al. 2010; Polumbryk et al. 2013; Iskra and Vlizlo 2013; Chekman et al. 2014; Reznikov et al. 2014).

A special place among doxorubicin-based prodrugs is taken by its conjugates with the noble metal nanoparticles, primarily Au. A high surface-to-volume ratio inherent to nanoparticles enables rapid response kinetics and provides improved drug-loading capabilities. In addition, gold nanoparticles (AuNPs) provide a high degree of biocompatibility and controlled synthesis. For gold nanoparticles, a wide range of optical absorption bands exists, the presence of which is due to localized surface plasmon resonance (LSPR) phenomenon. Particularly, for a colloidal solution of gold nanoparticles with dimensions much smaller than the wavelength of incident light, the absorption band corresponds to transverse LSPR and is located in the spectral range of 500–600 nm. The absorption band, located in the region of the therapeutic window of the transparency of biological tissues at 800–900 nm, corresponds to longitudinal LSPR on elongated nanoparticles (nanorods). In general, LSPR band can be shifted to the region of longer or shorter wavelengths, taking into account that the absorption wavelength of the electromagnetic field energy, which is associated with the collective oscillations of free electrons on the surface of the nanoparticle, depending on size and shape of the nanoparticles, distance between them, whether they are combined into clusters or arrays, especially ordered, and also on the properties of a adjacent dielectric medium (Meshalkin and Bgatova 2008). LSPR spectra are very sensitive to changes in these characteristics of nanostructures and dielectric permittivity of their environment and, therefore, they are capable of reacting to processes of electron-conformational transformations in molecules of drugs, including their complexation with antioxidants. In addition, nanoparticles can heat up due to light absorption, providing thermal effects on tumor cells, and serve as containers for transport and release of drugs in malignant tumors (Lal et al. 2007; Zhou et al. 2007; Liu et al. 2007; Khlebtsov 2008; Anker et al. 2008, 2009; Murray et al. 2009; You et al. 2010; Yeshchenko et al. 2016; Daraee et al. 2016). An important factor in the expediency of using gold nanoparticles as nanocontainers for medicinal products is the stability of a nanoparticle–drug system, which eliminates the effects of aggregation with the subsequent withdrawal of aggregates by a macrophage system leading to a reduction or complete cancellation of the therapeutic effect of drugs.

Antioxidant drugs administered to the body to reduce the harmful effect of Dox include BSA, one of the transport proteins (Peters 1985). It is known that a free sulfide group, which occurs in 70% of albumin molecules, participates in disulfide exchange with the formation of intermolecular complexes and has a Dox effect (Gorchakova et al. 2011). It is known that BSA also forms complexes with Dox (Gorchakova et al. 2011; Honary et al. 2010). It is obvious that physical interaction in BSA complexes with doxorubicin is accompanied by electron-conformational transformations in the molecules of the drug itself. Similar formation of complexes takes place in conjugates of BSA and Dox with AuNPs. At the same time, to the best of our knowledge, the influence of gold nanoparticles on the processes of complexation between molecules of antitumor and antioxidant drugs has not been studied (Gautier et al. 2013).

In presented study, we select the pharmaceutical form of doxorubicin as the most often used form for such type of antibiotic. The purpose of this work is to investigate the physical interaction between doxorubicin and bovine serum albumin complex in the presence of gold nanoparticles and lactose.

Experimental

In this work, we used gold(III) chloride hydrate $HAuCl_4 \cdot xH_2O$ and sodium citrate tribasic dihydrate $Na_3C_6H_5O_7 \cdot 2H_2O$ (Sigma-Aldrich), drug formulation of doxorubicin (Pfizer) in the form of a powder mix of Dox with anhydrous lactose, containing 17% active substance, and bovine serum albumin of fraction V for biochemistry (Merck). Deionized water (Millipore) was titrated with a NaOH solution to a pH of 6.9. Preparation of solutions and all measurements were carried out at room temperature.

Measurements of pH were carried out using the pH meter EcoScan pH 5+ with a pH electrode FC7252101B and an automatic temperature compensation sensor. Measurements of the solutions light absorption spectra were performed using a two-channel UV–Vis–NIR spectrophotometer UNICO SpectroQuest 4802 (United Products and Instruments, Inc., USA) in the spectral range of 350–800 nm in 1 nm steps.

Preparation of solutions

As plasmon-generating structures we used colloidal solutions of gold nanoparticles with an average size of 13 nm with an absorption peak in the vicinity of 520 nm obtained as a result of citrate reduction of the gold salt (Fig. 1).

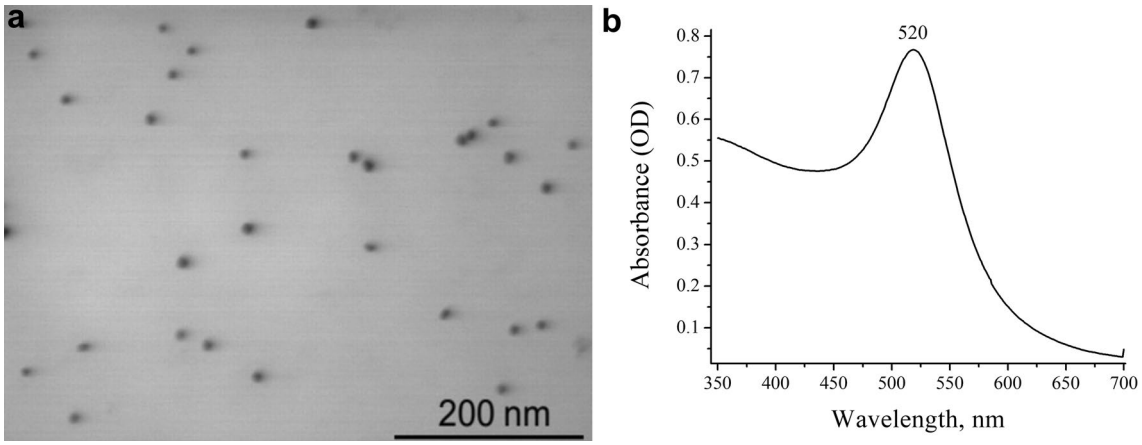

Fig. 1 **a** Transmission electron microscope image and **b** light absorption spectrum of colloidal AuNPs with a concentration of $C_{AuNPs} = 1.25$ nM. **a** Adapted with permission from Chegel V, Rachkov O, Lopatynskyi A, Ishihara S, Yanchuk I, Nemoto Y et al. (2012) Gold nanoparticles aggregation: drastic effect of cooperative functionalities in a single molecular conjugate. J Phys Chem C 116:2683–2690. Copyright 2012 American Chemical Society

For the synthesis of colloidal solutions of gold nanoparticles, the well-known Turkevich method was used (Turkevich et al. 1951; McFarland et al. 2004). 20 mL of 1 mM aqueous solution of gold(III) chloride hydrate was heated in a glass flask to boil under constant stirring. After boiling started, 2 mL of 38.8 mM aqueous solution of sodium citrate tribasic dihydrate was added to the flask and mixture continued to boil and stir with keeping constant liquid volume for 10 min until the solution acquired intense red color, which evidenced the completion of the formation of colloidal gold nanoparticles. Before use, the solution was cooled to room temperature. In this work, a colloidal solution of gold nanoparticles with a concentration of $C_{AuNPs} = 1.25$ nM was used.

The study of the interaction of Dox with BSA was carried out by adding to aqueous solution of Dox/lactose ($C_{Dox} = 1.77 \times 10^{-4}$ M in 3 mL aliquots) weighed portions of BSA so that the ratio of albumin to Dox concentrations varied from 0 to 1 (Table 1). The absorption spectrum for Dox/lactose solutions in plastic spectrophotometric cells was recorded in the visible region.

The concentration of Dox in the initial solutions and when using the Ostromislensky–Job method of isomolar series was determined spectrophotometrically. To prepare the starting solution, 6.4 mg of Dox/lactose was diluted in 10 mL of deionized water (pH 6.9). Given that the content of the pure substance of Dox in the powder is 17%, and the measured optical density of the solution obtained at $\lambda = 481$ nm is 2, the concentration of Dox is $C_{Dox} = 2 \times 10^{-4}$ M, taking into account the almost complete absence of lactose absorption at the respective band of Dox (Fiorante et al. 2015). Further, the initial solution was diluted with deionized water to obtain Dox solutions with necessary concentrations. Optical absorption spectra were determined for all solutions necessary for conducting an isomolar series of measurements. To Dox/lactose solutions, weighed portions of BSA with appropriate concentrations of C_{BSA} were added so that for the various C_{BSA}/C_{Dox} ratios, the total concentration of substances in the solution remained constant and amounted to 2×10^{-4} M (Table 2).

Results and discussion

Doxorubicin (Fig. 2a, b) exists in different prototropic forms, depending on the protonation of the functional groups (Sturgeon and Schulman 1977). In the case of the protonation of carbonyl and alkyl amino groups, the basic form becomes a double-charged cation. When protonation is taken place only to the alkyl amino group, a single-charged cation form appears. It is also possible that two

Table 1 Weighed portions and concentrations of BSA and BSA/Dox concentration ratios in solutions

Mass and concentrations	Sample number							
	1	2	3	4	5	6	7	8
m_{BSA}, mg	0	3.6	6.9	10.5	14.1	17.4	24.6	35.1
C_{BSA}, 10^{-5} M	0	1.77	3.54	5.31	7.08	8.85	12.39	17.7
C_{BSA}/C_{Dox}	0	0.1	0.2	0.3	0.4	0.5	0.7	1

Table 2 Weighed portions, concentrations of solution components and their ratios while keeping the total concentration $C_{BSA}+C_{Dox}=2\times10^{-4}$ M

Mass, concentrations and their ratios	Sample number										
	1	2	3	4	5	6	7	8	9	10	11
m_{BSA}, mg	39.6	34.9	31.8	27.6	23.7	19.8	15.9	13.5	11.7	4.3	0
C_{BSA}, 10^{-4} M	2	1.8	1.6	1.4	1.2	1	0.8	0.68	0.6	0.2	0
C_{Dox}, 10^{-4} M	0	0.2	0.4	0.6	0.8	1	1.2	1.32	1.4	1.8	2
C_{BSA}/C_{Dox}	–	9:1	8:2	7:3	6:4	5:5	4:6	1:2	3:7	1:9	0
$C_{Dox}/(C_{Dox}+C_{BSA})$	0	0.1	0.2	0.3	0.4	0.5	0.6	0.66	0.7	0.9	1

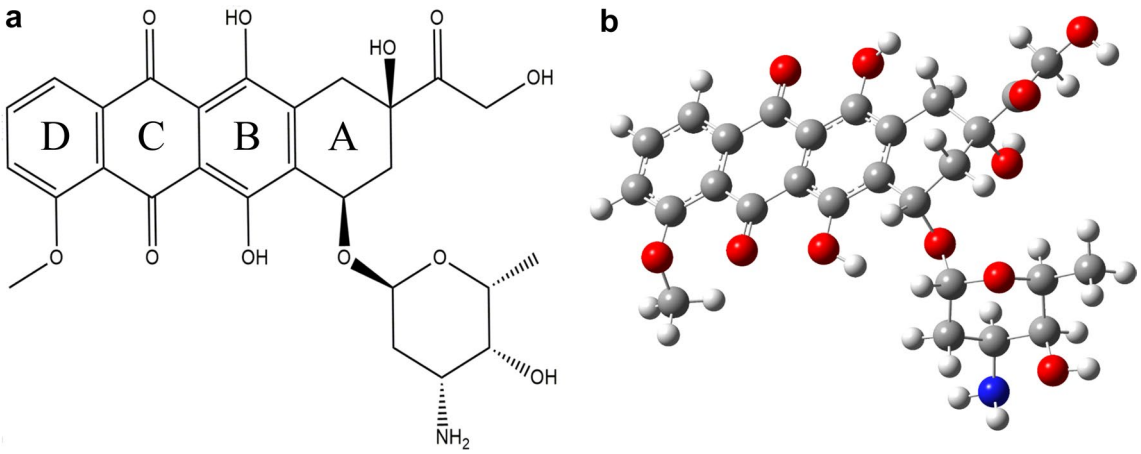

Fig. 2 **a** The molecular structure and **b** atomic structure for the main prototropic form of Dox (National Center for Biotechnology Information 2005)

protons split from phenolic groups with the occurrence of a double-charged anion or, if only one proton is detached, a single-charged anion appears. If the proton is cleaved from the phenol group, and the proton is connected to the alkyl amino group, then zwitterion appears. Depending on the type of prototropic form, the positions of the maxima of optical absorption, fluorescence and the magnitudes of molar extinction coefficients significantly change.

The Dox molecule exhibits a tetrahydrotetracene-quinone chromophore, consisting of an alicyclic ring A and three six-membered coplanar aromatic rings B, C, D. The chromophore is bound to one or more monosaccharide residues. The carbohydrate residue is 2,3,6-trideoxy-3-amino-L-lixo-hexapyranose (daunosamine). The aglyconic portion of the molecule includes the radical R=CH_2–OH. The indicated structure, depending on the considered components, allows Dox to exhibit amphiphilic (hydrophilic and lipophilic) and amphoteric (ionic) properties, and, consequently, to cover hydrophilic, lipophilic materials, as well as to be bound to materials as a result of the implementation of hydrophobic, hydrogen interactions and ion exchange as a result of protonation (Gautier et al. 2013; Pawar et al. 2012; Pawar and Vavia 2015; Tian et al. 2015). It should be noted that the molecular weight of Dox is 543.5 g/mol.

The molecular structure of BSA includes three amide domains with different charge values at a total negative charge of − 18 at a neutral pH. With a total amount of amino acids equal to 582, BSA comprises 19 tyrosine residues, 27 phenylalanine residues and two tryptophan residues, which lead to the appearance of fluorescence in the ultraviolet region of the spectrum at a pronounced absorption band of about 280 nm. The molecular weight of BSA is 66,267 g/mol (Peters 1985).

The lactose in pharmaceutical form of doxorubicin is a lyoprotectant molecule that, when combined with the Dox, substantially reduces the chemical and physical instability of the antibiotic during lyophilization and subsequent storage. It is obvious that this sugar cannot induce any noticeable structural changes in the Dox molecule. Recently, the interactions of the lactose with BSA were investigated (Zhang et al. 2016) using fluorescence, FTIR and circular dichroism techniques. The results indicated that lactose has almost no effect on the structure of the BSA and cannot be directly bonded by protein. Also, knowing that molecular weight of lactose is very small (342.3 g/mol), and, together with known absence of its absorbance within the Dox absorption band, the influence of lactose on the studied BSA/Dox absorbance spectra is quite minimal and, in our opinion, can be neglected.

Figure 3 shows optical absorption spectra for Dox/lactose–BSA solutions with different content of protein molecules, according to Table 1, at a constant concentration of doxorubicin equal to 1.77×10^{-4} M. For aqueous Dox solution with a concentration of 1.77×10^{-4} M, the maximum optical density position is located near $\lambda = 481$ nm. The location of the absorption peak near $\lambda = 481$ nm indicates that Dox molecules are in the prototropic form of a single-charged cation in the presence of a proton connected to the alkyl amino group (Sturgeon and Schulman 1977). When albumin is added to the Dox/lactose solution, the peak position is slightly (~2 nm) shifted in the long-wave direction. In addition, the shape of the absorption band changes. Obviously, such a transformation of the spectra of Dox/lactose–BSA solutions is caused by changes in the conformational state of the antibiotic and is a consequence of complex formation. The formation of complexes is also confirmed by the nature of decreasing the optical density at the position of the maximum absorption of the solution for different ratios of concentrations C_{BSA}/C_{Dox} (Fig. 4a). It is evident that with increasing BSA content, the optical density falls as a result of the formation of complexes between doxorubicin and albumin molecules, which is accompanied by a decrease in the number of free drug molecules that are not bound in the complexes, and a decrease in the magnitude of the molar extinction coefficient of complexes ε_K. For these minimum values of optical density in a solution, a dynamic equilibrium is established between the concentrations of free molecules and those bound in complexes.

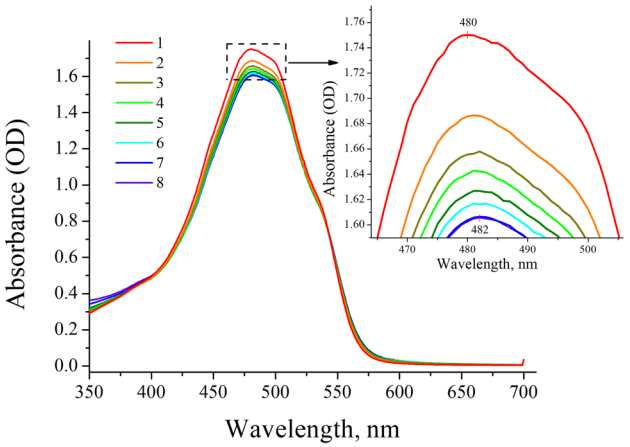

Fig. 3 Optical density spectra of Dox–BSA solutions in water (pH 6.9) for a constant concentration of Dox (1.77×10^{-4} M) and containing 0 M (1), 1.77×10^{-5} M (2), 3.54×10^{-5} M (3), 5.31×10^{-5} M (4), 7.08×10^{-5} M (5), 8.85×10^{-5} M (6), 1.239×10^{-4} M (7), 1.77×10^{-4} M (8) BSA. Inset: parts of spectra in the wavelength range near $\lambda = 481$ nm

Formation of complexes presupposes the existence of a definite number of binding sites. The number of binding sites for n molecules of Dox and protein can be determined by measuring the isomolar series. The method of isomolar series involves the study of the dependence of the difference of optical densities $A_0 - A$ measured at the position of the maximum absorption of Dox ($\lambda = 481$ nm), where A_0 and A are the optical densities of Dox solutions in the absence of BSA and in the presence of BSA, respectively, on the ratio of concentrations $C_{BSA}/(C_{BSA} + C_{Dox})$. The total concentration $C_{BSA} + C_{Dox}$ for all solutions remained the same and equaled 2×10^{-4} M. The concentrations of the components were selected with certain ratios of C_{BSA}/C_{Dox} (Table 2).

Figure 4b shows the dependence of the difference of optical densities $A_0 - A$ on the ratio of concentrations $C_{BSA}/(C_{BSA} + C_{Dox})$. It is seen that the maximum difference in optical

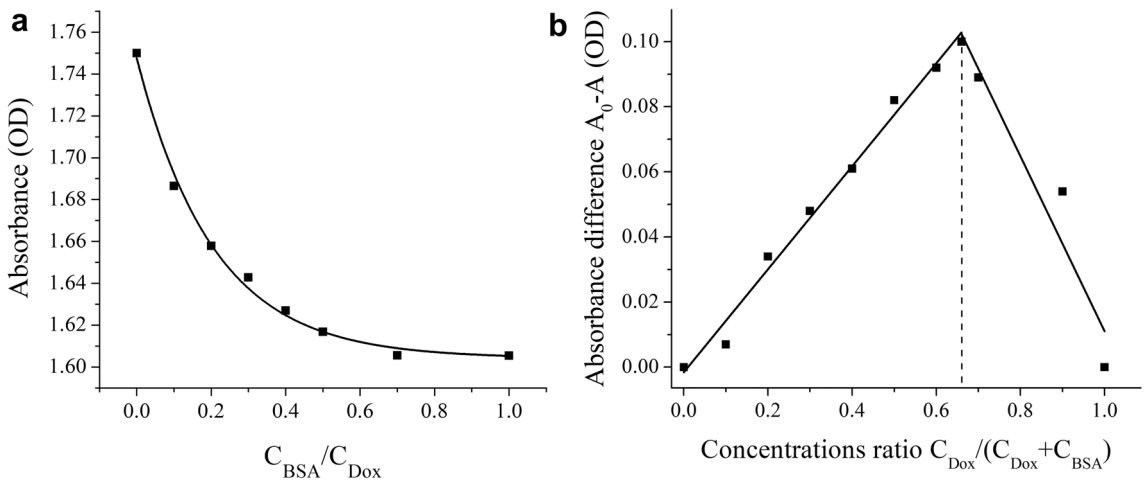

Fig. 4 **a** Dependence of the optical density of Dox–BSA solutions at the absorption maximum on the ratio of concentrations C_{BSA}/C_{Dox}. **b** Dependence of difference of optical densities of Dox–BSA aqueous solutions on the ratio of their concentrations, which is presented in accordance with the method of isomolar series ($C_{BSA} + C_{Dox} = 2 \times 10^{-4}$ M)

densities is near the value of $C_{BSA}/(C_{BSA}+C_{Dox})\approx 0.66$, which corresponds to the ratio $C_{BSA}/C_{Dox}=1{:}2$. This result indicates that in the Dox–BSA complex two Dox molecules and one albumin molecule are bound, that is, there are two sites of binding of the antibiotic molecules to the BSA macromolecule ($n=2$).

Establishing the number of binding sites allows us to write the equation of the equilibrium state of formation and dissociation of the considered complexes in the form:

$$2[D]+[B]\overset{[K]}{\leftrightarrow}[D_2B], \tag{1}$$

where $[D]$, $[B]$, $[D_2B]$ are the concentrations of free molecules of Dox and albumin and those in the complexes, respectively, K is the stability (binding) constant of the complex. Taking into account the obtained value $n=2$, the specified stability (dynamic equilibrium) constant can be determined as follows (Gorchakova et al. 2011; Yatsymirskyy and Vasiliev 1959):

$$K=\frac{[D_2B]}{[D]^2\cdot[B]}. \tag{2}$$

The concentrations of free (unbound in complexes) molecules can be written as follows:

$$[D]=D_0-2\cdot[D_2B], \tag{3}$$

$$[B]=B_0-[D_2B]. \tag{4}$$

Complex formation with the ratio of the components of $C_{BSA}/C_{Dox}=1{:}2$ is realized at initial concentrations $D_0=1.32\times10^{-4}$ M and $B_0=0.68\times10^{-4}$ M.

As already noted, the optical density of the Dox solution with albumin depends not only on the concentration of free antibiotic molecules $[D]$, but also on the concentration of complexes $[D_2B]$ and the corresponding molar extinction coefficients ε_0 and ε_K, which can be written as:

$$A=\varepsilon_0\cdot[D]+\varepsilon_K\cdot[D_2B]. \tag{5}$$

If the concentration of BSA goes to infinity, then the concentration of free Dox molecules decreases to zero, since they will all be in complexes. This allows determining the value of A_K, which corresponds to the absorption of light by complexes at $\lambda=481$ nm, from the dependence of optical density on inverse BSA concentration $1/C_{BSA}$. Figure 5 shows the specified dependence for samples, the concentration of C_{BSA} in which is shown in Table 1.

Extrapolation of this dependence to $1/C_{BSA}\to 0$ ($C_{BSA}\to\infty$) indicates that the optical density A_K due to the light absorption by Dox molecules in complexes at $\lambda=481$ nm is approximately 1.6. Accordingly, the molar extinction coefficient of complexes can be determined from the expression:

$$\varepsilon_K=\frac{A_K}{C_{Dox}}\approx 9045. \tag{6}$$

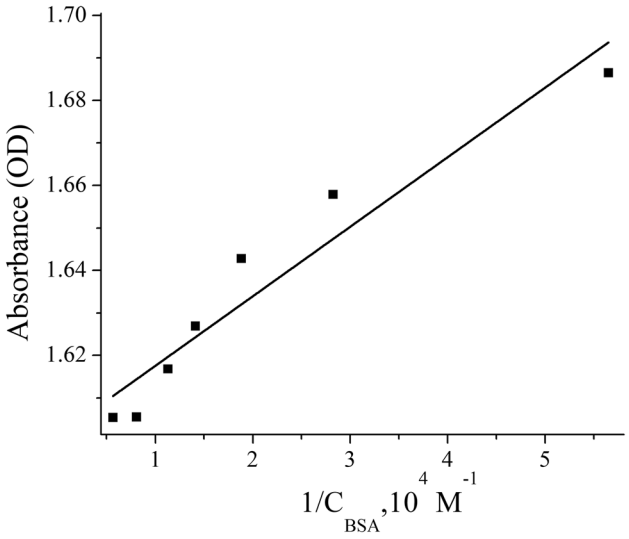

Fig. 5 Dependence of the optical density of Dox–BSA solutions on inverse BSA concentration $1/C_{BSA}$

The obtained value for the complex is smaller in comparison with the molar extinction coefficient of Dox solution, which confirms the nature of the change in optical density in Fig. 4a. Using the Eqs. (2)–(5) and known values $D_0=1.32\times10^{-4}$ M, $B_0=0.68\times10^{-4}$ M, $\varepsilon_0=9932$, $\varepsilon_K=9045$, $A_K=1.6$, we can obtain the calculated value of the binding constant $K=7.56\times10^6$ M^{-2} or $\log_{10}K=6.88$.

The result of significant binding between Dox and BSA molecules is confirmed by studying the fluorescence of albumin solution with a constant concentration of 10^{-5} M and different contents of Dox (Bi et al. 2009). In addition to fluorescence quenching, the maximum of which for BSA corresponds to about 342 nm ($\lambda_{ex}=280$ nm) due to radiation from the amino acid residues of tryptophan, there is also a redshift of the emission band, which is determined by the hydrophobic environment of tryptophan. The results obtained by the authors indicate that the main contribution to the binding between BSA and Dox molecules belongs to the hydrophobic effect.

It is obvious that in the presence of spherical gold nanoparticles in Dox–BSA solutions one can expect changes in the constant of the dynamic equilibrium K at complex formation due to its photoactivation via LSPR. The effect on the specified constant allows for the change in the number of free molecules of Dox as a factor that, on the one hand, is important for the neutralization of tumor cells, and, on the other hand, it can reduce the effect of apoptosis of normal cells.

Figure 6 shows the optical density spectra for solutions of pure Dox and Dox–BSA conjugates with gold nanoparticles. Upon the addition of AuNPs, a new band at about 498 nm appears that corresponds to the Dox–AuNPs conjugate. With

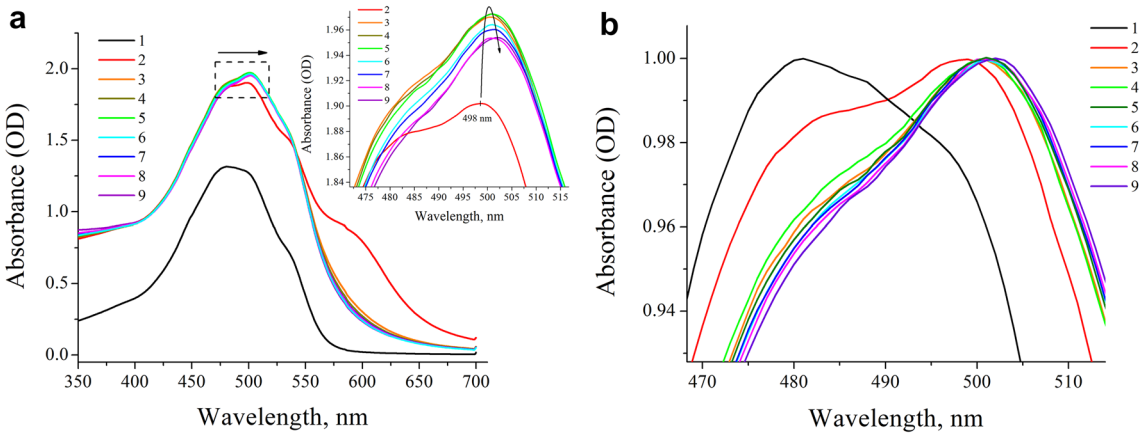

Fig. 6 **a** Optical density spectra of solutions of Dox (1.33×10^{-4} M) (1), Dox conjugates with AuNPs (2) and Dox with 1.33×10^{-5} M (3), 2.66×10^{-5} M (4), 3.98×10^{-5} M (5), 5.31×10^{-5} M (6), 6.64×10^{-5} M (7), 9.29×10^{-5} M (8), 13.3×10^{-5} M bovine serum albumin (9) with gold nanoparticles at a concentration of 1.25 nM. Inset: parts of spectra in the wavelength range near $\lambda = 481$ nm. **b** Parts of the same normalized spectra in the wavelength range near $\lambda = 481$ nm

adding of the lowest concentration of BSA (1.33×10^{-5} M), upon creation of gold nanoparticles conjugates with Dox and albumin solutions, the spectral reconstruction of optical absorption is observed with preserving a doxorubicin-specific band near $\lambda = 481$ nm and sharp increasing of optical density. The band at 498 nm shifts with growing BSA concentration to a maximum at about $\lambda = 500$ nm followed by a slight optical density decrease (Fig. 6a, inset). Changes in this part of the spectrum are more likely to be the result of conformational changes in the Dox molecule. Creating conjugates of protein and antibiotic with gold nanoparticles leads to a substantial visible rearrangement of the right side of the optical density spectrum of Dox molecule, which may be due to both the change in the Dox conformation and the aggregation of gold nanoparticles. Since the stabilization of gold nanoparticles in an aqueous solution is provided by a layer of citrate, which leads to the appearance of negative charges on their surface, the coating of AuNPs with Dox molecules in monocationic prototropic form is considered as a result of electrostatic interaction. The magnitude of such binding essentially depends on the pH of medium surrounding the resulting conjugates and is manifested as the red shift of the resonant band characteristic to AuNPs at about 520 nm and the emergence of new optical absorption bands in the range up to 700 nm, if aggregation of nanoparticles is observed (Chegel et al. 2012).

Aggregation of gold nanoparticles with their subsequent precipitation is most likely due to the loss of stabilizing properties of citrate coating as a result of the transfer of protons with a change in the prototropic form of Dox. Indeed, in accordance with (Chegel et al. 2012), only compounds with highly protonated amino groups and at high concentrations can neutralize the negative charge of citrate-stabilized AuNPs with subsequent aggregation. The Dox molecule has an amino group, but under conditions of neutral pH its presence cannot be a key factor in destabilizing the colloidal solution and initiating the aggregation process. However, the addition of colloidal gold with pH 5 changes the acidity of a neutral solution of Dox, which leads to the protonation of the Dox molecule and the aggregation of gold nanoparticles. The indicated protonation is also evidenced as the displacement of the peak of the vibrational mode of the amino group at a frequency of 3777 cm^{-1}–3373 cm^{-1} position in the FTIR spectrum (Mirza and Shamshad 2011). That is, the aggregation process in our case may be due to the charge transfer process in the Dox–AuNPs conjugate, which is accompanied by spectral changes in the Dox molecule, characteristic of the anionic prototropic form of doxorubicin. The calculation of the difference between the optical densities obtained for Dox solutions with AuNPs ($A_{\text{Dox+AuNPs}}$) and the sum of the optical densities of constituents $A_{\text{Dox}} + A_{\text{AuNPs}}$ reveals an intense absorption band located at $\lambda = 600$ nm (Fig. 7). It can be assumed that this band is characteristic to the anionic prototropic form of doxorubicin (Sturgeon and Schulman 1977), the occurrence of which is due to the transfer of charges in the conjugate with subsequent aggregation of nanoparticles and their precipitation, which depends on the concentration of BSA in solutions.

In the presence of BSA in solution, this band gradually disappears and a new band near 550 nm appears (Fig. 7), which belongs to the cationic double-charged form of doxorubicin, that is, when the initial concentration of BSA increases, an anionic prototropic form of doxorubicin is transformed into its cationic double-charged form. At significant concentrations of protein in the presence of AuNPs, the most probable is the transition of Dox from a single-cationic prototropic form to a double-cationic form. Thus, protein molecules suspend the proton transfer process and

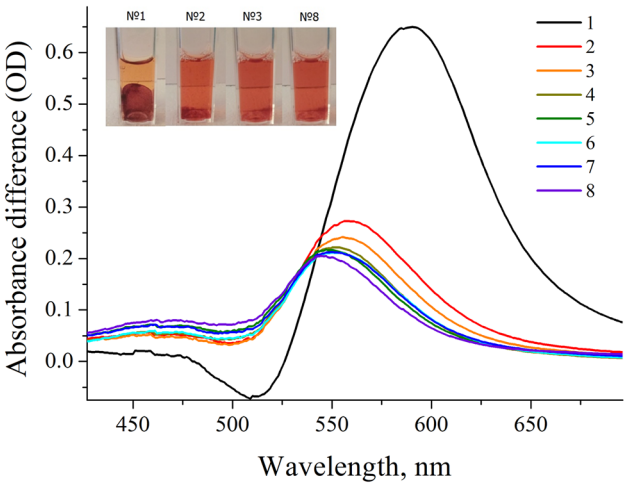

Fig. 7 Spectra of the optical densities difference $A_{Dox+AuNPs} - (A_{Dox} + A_{AuNPs})$ (1) and $A_{Dox+BSA+AuNPs} - (A_{Dox+BSA} + A_{AuNPs})$ at BSA concentrations of 1.33×10^{-5} M (2), 2.66×10^{-5} M (3), 3.98×10^{-5} M (4), 5.31×10^{-5} M (5), 6.64×10^{-5} M (6), 9.29×10^{-5} M (7), 13.3×10^{-5} M (8), 1.33×10^{-4} M Dox and 1.25 nM AuNPs. Inset: photograph of samples 1, 2, 3 and 8, where differences in precipitation of AuNP–Dox–BSA aggregates for samples with different BSA concentration are observed

play a stabilizing role in conjugates with AuNPs, forming not only C, but also D forms of antibiotic molecules, which contributes to the preservation of negative citrate-induced charges on their surfaces, and thus keeps AuNPs from aggregation. With increasing concentration of BSA, the precipitate of aggregated gold nanoparticles gradually disappears and at the highest content of 1.33×10^{-4} M is not observed (Fig. 7, inset).

The results presented not only evidence of the substantial binding between BSA and Dox with the formation of the complex, but also imply the significant effect of gold nanoparticles on the mechanism of complex formation and conformational changes in the protein–antibiotics system at LSPR conditions. That is, the presence of AuNPs enhances the regulatory capabilities of the Dox–BSA complex and can be used to create prodrugs.

Conclusions

The nature of the changes in the spectra of optical absorption of Dox antibiotic with the increase in the content of the protein macromolecules of bovine serum albumin in an aqueous solution indicates the complexation between components with a high binding constant $K = 7.56 \times 10^6$ M^{-2} and the number of binding sites $n = 2$. Such binding is explained by the presence of a hydrophobic interaction.

Dox conjugated with gold nanoparticles is characterized by appearance of a new intense absorption band located near $\lambda = 600$ nm. It can be assumed that the indicated band belongs to the anionic prototropic form of doxorubicin. In the presence of BSA in solution and with an increase in its concentration, this band disappears with a transformation in a band near 550 nm, which may belong to the cationic double-charged form of Dox.

When adding gold nanoparticles to Dox solutions with different albumin content, optical absorption spectra undergo significant changes due to a decrease in the interaction of an antibiotic with nanoparticles, a significant association of albumin molecules with AuNPs, and, as a consequence, the rearrangement of the Dox–BSA–AuNPs system to a more stable state, which is important in the drug delivery process.

The results of the study indicate the possibility of creating effective prodrugs comprising Dox–BSA–AuNPs with regulated properties of antibiotic and protein complexation due to the presence of AuNPs.

Compliance with ethical standards

Conflict of interest On behalf of all authors, the corresponding author states that there is no conflict of interest.

References

Anker JN, Hall WP, Lyandres O, Shah NC, Zhao J, Van Duyne RP (2008) Biosensing with plasmonic nanosensors. Nat Mater 7:442–453

Anker JN, Hall WP, Lambert MP, Velasco PT, Mrksich M, Klein WL et al (2009) Detection and identification of bioanalytes with high resolution LSPR spectroscopy and MALDI mass spectrometry. J Phys Chem C 113:5891–5894

Arcamone F (1981) Doxorubicin: anticancer antibiotics. Academic Press, New York

Bi S, Sun Y, Qiao C, Zhang H, Liu C (2009) Binding of several antitumor drugs to bovine serum albumin: fluorescence study. J Lumin 129:541–547

Carvalho FS, Burgeiro A, Garcia R, Moreno AJ, Carvalho RA, Oliveira PJ (2014) Doxorubicin-induced cardiotoxicity: from bioenergetic failure and cell death to cardiomyopathy. Med Res Rev 34:106–135

Cataldo F, Da Ros T (2008) Medicinal chemistry and pharmacological potential of fullerenes and carbon nanotubes. Springer, Dordrecht

Chegel V, Rachkov O, Lopatynskyi A, Ishihara S, Yanchuk I, Nemoto Y et al (2012) Gold nanoparticles aggregation: drastic effect of cooperative functionalities in a single molecular conjugate. J Phys Chem C 116:2683–2690

Chekman IS, Belenichev IF, Gorchakova NA, Kucherenko LI, Bukhtiyarova NV, Pogotova GA (2014) Antioxidants: clinical and pharmacological aspects. Ukr Med J 1:22–28 **(in Russian)**

Chen Z, Mao R, Liu Y (2012) Fullerenes for cancer diagnosis and therapy: preparation, biological and clinical perspectives. Curr Drug Metab 13:1035–1045

Dallavalle M, Leonzio M, Calvaresi M, Zerbetto F (2014) Explaining fullerene dispersion by using micellar solutions. ChemPhysChem 15:2998–3005

Daraee H, Eatemadi A, Abbasi E, Fekri Aval S, Kouhi M, Akbarzadeh A (2016) Application of gold nanoparticles in biomedical and drug delivery. Artif Cells Nanomed Biotechnol 44:410–422

Dellinger A, Zhou Z, Connor J, Madhankumar AB, Pamujula S, Sayes CM et al (2013) Application of fullerenes in nanomedicine: an update. Nanomedicine 8:1191–1208

Durackova Z (2010) Some current insights into oxidative stress. Physiol Res 59:459–469

Dykman LA, Bogatyrev VA, Shchyogolev SU, Khlebtsov NG (2008) Gold nanoparticles: synthesis, properties, biomedical application. Nauka, Moscow **(in Russian)**

Evstigneev MP, Buchelnikov AS, Voronin DP, Rubin YV, Belous LF, Prylutskyy YI et al (2013) Complexation of C_{60} fullerene with aromatic drugs. ChemPhysChem 14:568–578

Fiorante PF, Martins RD, Palma MSA (2015) Development and validation of analytical methodology with focus on the qualification of powder mixers. Braz J Pharm Sci 51:273–284

Gautier J, Allard-Vannier E, Munnier E, Soucé M, Chourpa I (2013) Recent advances in theranostic nanocarriers of doxorubicin based on iron oxide and gold nanoparticles. J Control Release 169:48–61

Gorchakova NO, Chekman IS, Vlasova NM, Golovkova LP, Gerashenko II, Maximchuk OO (2011) Doxorubicin complexation with bovine serum albumin. Rep Natl Acad Sci Ukr 4:177–181 **(in Ukrainian)**

Honary S, Jahanshahi M, Golbayani P, Ebrahimi P, Ghajar K (2010) Doxorubicin-loaded albumin nanoparticles: formulation and characterization. J Nanosci Nanotechnol 10:7752–7757

Iskra RJ, Vlizlo VV (2013) Peculiarities of antioxidant defense system in erythroid cells and tissues of pigs under action of chromium chloride. Ukr Biochem J 85:96–102 **(in Ukrainian)**

Kalinkina NV (2004) Anthracycline cardiomyopathy. Ukr J Cardiol 2:112–116 **(in Russian)**

Khlebtsov NG (2008) Optics and biophotonics of nanoparticles with a plasmon resonance. Quantum Electron 38:504

Krohn K (1983) Book review: anthracycline antibiotics. Edited By H. S. El Khadem. Angew Chem Int Ed Engl 22:895–896

Lal S, Link S, Halas NJ (2007) Nano-optics from sensing to waveguiding. Nat Photonics 1:641–648

Liu X, Atwater M, Wang J, Huo Q (2007) Extinction coefficient of gold nanoparticles with different sizes and different capping ligands. Colloids Surf B Biointerfaces 58:3–7

Lobo V, Patil A, Phatak A, Chandra N (2010) Free radicals, antioxidants and functional foods: impact on human health. Pharmacogn Rev 4:118–126

McFarland AD, Haynes CL, Mirkin CA, Van Duyne RP, Godwin HA (2004) Color my nanoworld. J Chem Educ 81:544A

Meshalkin YP, Bgatova NP (2008) Prospects and problems of the use of inorganics nanoparticles in oncology. J Sib Fed Univ Biol 3:248–268 **(Review) (in Russian)**

Mirza AZ, Shamshad H (2011) Preparation and characterization of doxorubicin functionalized gold nanoparticles. Eur J Med Chem 46:1857–1860

Montellano A, Da Ros T, Bianco A, Prato M (2011) Fullerene C_{60} as a multifunctional system for drug and gene delivery. Nanoscale 3:4035–4041

Mosunov AA, Pashkova IS, Sidorova M, Pronozin A, Lantushenko AO, Prylutskyy YI et al (2017) Determination of the equilibrium constant of C_{60} fullerene binding with drug molecules. Phys Chem Chem Phys 19:6777–6784

Murray WA, Auguié B, Barnes WL (2009) Sensitivity of localized surface plasmon resonances to bulk and local changes in the optical environment. J Phys Chem C 113:5120–5125

National Center for Biotechnology Information (2005) Doxorubicin. PubChem Open Chemistry Database. https://pubchem.ncbi.nlm.nih.gov/compound/31703. Accessed 24 Mar 2018

Orel V, Romanov A, Rykhalskyi O, Shevchenko A, Orel I, Burlaka A et al (2016) Antitumor effect of superparamagnetic iron oxide nanoparticles conjugated with doxorubicin during magnetic nanotherapy of Lewis Lung carcinoma. Materialwiss Werkstofftech 47:165–171

Pawar SK, Vavia P (2015) Efficacy interactions of PEG–DOX–*N*-acetyl glucosamine prodrug conjugate for anticancer therapy. Eur J Pharm Biopharm 97:454–463

Pawar SK, Badhwar AJ, Kharas F, Khandare JJ, Vavia PR (2012) Design, synthesis and evaluation of *N*-acetyl glucosamine (NAG)–PEG–doxorubicin targeted conjugates for anticancer delivery. Int J Pharm 436:183–193

Peters T Jr (1985) Serum albumin. Adv Protein Chem 37:161–245

Polumbryk M, Ivanov S, Polumbryk O (2013) Antioxidants in food systems. Mechanism of action. Ukr J Food Sci 1:15–40

Prylutskyy YI, Evstigneev MP, Pashkova IS, Wyrzykowski D, Woziwodzka A, Gołuński G et al (2014) Characterization of C_{60} fullerene complexation with antibiotic doxorubicin. Phys Chem Chem Phys 16:23164–23172

Prylutskyy YI, Evstigneev MP, Cherepanov VV, Kyzyma OA, Bulavin LA, Davidenko NA et al (2015) Structural organization of C_{60} fullerene, doxorubicin, and their complex in physiological solution as promising antitumor agents. J Nanopart Res 17:45

Reznikov OH, Polumbryk OM, Balion YH, Polumbryk MO (2014) Pro- and antioxidant systems and pathological processes in humans. Visn Nac Akad Nauk Ukr 10:17–29 **(in Ukrainian)**

Sturgeon RJ, Schulman SG (1977) Electronic absorption spectra and protolytic equilibria of doxorubicin: direct spectrophotometric determination of microconstants. J Pharm Sci 66:958–961

Tevyashova AN (2014) Creation of anthracycline prodrugs. Vestnik MITHT 9:11–25 **(in Russian)**

Tian B, Ding Y, Han J, Zhang J, Han Y, Han J (2015) *N*-Acetyl-D-glucosamine decorated polymeric nanoparticles for targeted delivery of doxorubicin: synthesis, characterization and in vitro evaluation. Colloids Surf B Biointerfaces 130:246–254

Turkevich J, Stevenson PC, Hillier J (1951) A study of the nucleation and growth processes in the synthesis of colloidal gold. Discuss Faraday Soc 11:55–75

Wang Q, Zhong YJ, Yuan JP, Shao LH, Zhang J, Tang L et al (2013) Targeting therapy of hepatocellular carcinoma with doxorubicin prodrug PDOX increases anti-metastatic effect and reduces toxicity: a preclinical study. J Transl Med 11:192

Yatsymirskyy KB, Vasiliev VP (1959) The instability constants of complex compounds. Publishing House of the USSR Academy of Sciences, Moscow **(in Russian)**

Yeshchenko OA, Kutsevol NV, Naumenko AP (2016) Light-induced heating of gold nanoparticles in colloidal solution: dependence on detuning from surface plasmon resonance. Plasmonics 11:345–350

You J, Shao R, Wei X, Gupta S, Li C (2010) Near-infrared light triggers release of paclitaxel from biodegradable microspheres: photothermal effect and enhanced antitumor activity. Small 6:1022–1031

Zhang Q, Ni Y, Kokot S (2016) Competitive interactions between glucose and lactose with BSA: which sugar is better for children? Analyst 141:2218–2227

Zhong YJ, Shao LH, Li Y (2013) Cathepsin B-cleavable doxorubicin prodrugs for targeted cancer therapy. Int J Oncol 42:373–383 **(Review)**

Zhou Y, Xu H, Dahlin AB, Vallkil J, Borrebaeck CAK, Wingren C et al (2007) Quantitative interpretation of gold nanoparticle-based bioassays designed for detection of immunocomplex formation. Biointerphases 2:6–15